

Lasers in Manufacturing Conference 2017

Selective laser melting of AlSi40 using ultrashort laser pulses for additive manufacturing applications

T. Ullsperger^{a,*}, G. Matthäus^a, L. Kaden^a, M. Rettenmayr^b, S. Risse^c, A. Tünnermann^{a,c}, S. Nolte^{a,c}

^a*Institute of Applied Physics, Abbe Center of Photonics, Friedrich-Schiller-Universität Jena, Albert-Einstein-Strasse 15, 07745 Jena, Germany*

^b*Otto Schott Institute of Materials Research, Friedrich-Schiller-Universität Jena, Löbdergraben 32, 07743 Jena, Germany*

^c*Fraunhofer Institute for Applied Optics and Precision Engineering, Albert-Einstein-Strasse 7, 07745 Jena, Germany*

Abstract

The additive manufacturing of specific material compositions like hypereutectic alloys reveals fundamental problems. In particular, during the fabrication with continuous wave lasers, the cooling rate is too low, resulting in a decomposition of the different material components and a limited precision due to the increased melting zone, respectively. In this work we demonstrate the selective laser melting of hypereutectic AlSi40 using 500 fs laser pulses at a wavelength of 1030 nm. A controlled heat accumulation was utilized to address different melting regimes. It was possible to reduce the structure size down to 50µm which is basically only limited by the grain size and layer thickness. Moreover, ultrashort laser pulses allow melting and re-solidification on extremely short timescales which leads to a non-thermal equilibrium processing. As a consequence, a more homogeneous micro-structure of AlSi40 can be demonstrated.

Keywords: Selective laser melting; Additive manufacturing; Light-weight structures; Ultra-short laser pulses; Hypereutectic alloys.

1. Motivation and State of the Art

Selective laser melting (SLM) of aluminum powders and corresponding alloys is used in a wide field of applications for instance in automotive and aerospace to fabricate casts and light-weight elements with a superior and complex structure that can't be produced with conventional machining techniques [1, 2]. In this context silicon is used to reinforce the material and decrease the thermal expansion [3]. However, the

* E-mail address: tobias.ullsperger@uni-jena.de .

cooling rate in conventional CW-laser-molten alloys with a high Si content, e.g. 40wt%, is too low, which leads to a decomposition due to low solubility of Si in Al. The result is the formation of large primary Si particles that reduces the local thermal and mechanical properties drastically [4, 5]. In addition the achieved minimal structure sizes for only single tracks are up to now in the range of 150 μm using laser micro-cladding of hypereutectic AlSi powder [6, 7].

To overcome these limitations, we are using ultra-short laser pulses as an alternative heating source. Ultra-short laser pulses in the range of femtoseconds to picoseconds are commonly used in laser material processing for nearly damage-free micro-ablation with a low heat-affected zone [8, 9]. In contrast to that, heat accumulation depending on the repetition rate and the thermal properties of the material can be specifically utilized, e.g. for the local welding of glass [10, 11]. Until now only a few groups have applied femtosecond laser pulses for the additive manufacturing of materials with high melting temperature, like tungsten and zirconium by using high repetitive laser systems [12-15]. Here, we make use of heat accumulation and the extraordinary short interaction time of the laser pulses with the material to realize a non-thermal equilibrium process for the additive manufacturing of hypereutectic AlSi. Apart from a fundamental analysis our approach aims at the production of customized light-weight elements with high ultimate tensile strength and highly resolved geometries.

2. Experimental Setup and Methodology

The experiments were realized with a manual SLM-device that enables the layer-wise melting in a powder bed which is shown in Fig. 1. For this purpose we used a femtosecond laser by Activefiber Systems GmbH

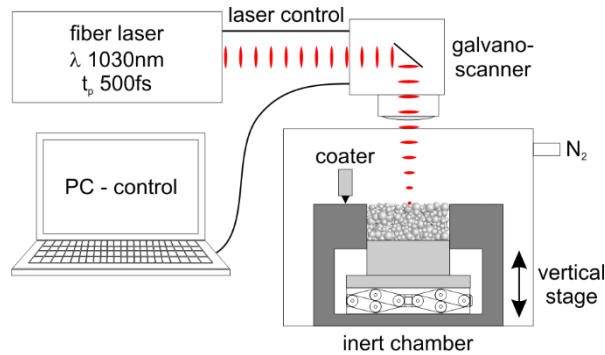


Fig. 1. Schematic representation of the manual SLM-setup.

that emits pulses with a central wavelength of 1030nm and a duration of 500fs. The maximum average power is 30W at a repetition rate of 20MHz. An external acousto-optic modulator can tune the repetition rate and operates as a shutter during a jump between two separate scanned paths. The pulses are deflected by a galvano scanner system (SCANgine, Scanlab) controlled with a computer program and focused then by a 100mm f-theta lens on the surface of the powder bed. The 1/e²-waist diameter was 35 μm . To avoid oxidation during the melting process a sealed chamber was built up and flooded with nitrogen. The residual oxygen level has been kept under 0.5%. The powder was deposited manually with a rubber blade on an aluminum building platform that was moved stepwise with the help of a vertical axis. In every single step, the powder layer with a thickness between 25 μm to 50 μm has a direct thermal contact to the building platform or previously molten material.

The powder material was pre-alloyed AlSi40 from TLS-Technik. After gas atomization of the melt in argon atmosphere sphere-like grains with a size distribution of 20-63 μm were generated. The fraction has been

sieved once again with a strainer mesh size of 40 μ m to obtain a lower particle size that nearly fits the spot diameter.

After appropriate parameter studies the additive manufactured samples were characterized by different microscopic methods, like light microscopy, scanning electron microscopy (SEM) and laser scanning microscopy (LSM) to qualify the melting characteristics and to quantify track widths and structure heights. Furthermore, to reveal a deeper insight into the microstructural features, the samples were mounted in epoxy resin and grounded on SiC paper up to 2400 grit. Then they were roughly polished with a diamond suspension and fine polished with an Al₂O₃ suspension (50nm grain size).

The energy transfer from the ultra-short laser pulses to the material is more complex and has higher degrees of freedom in comparison to continuous wave lasers. In general, basic SLM studies with cw lasers were performed by only varying the applied power, spot diameter and scanning speed except of the built orientation and different scan strategies. In contrast to that ultra-short laser pulses have a peak power, pulse energy, time duration, repetition (pulse) rate and concerning the wavelength and focusing conditions a nonlinear absorption characteristic regarding different materials, like silicon. For the comparison presented here, we limited and selected the variation of parameters. The pulse energy (E_p) and scanning speed (v_{scan}) were tuned while the repetition rate, the spot diameter on the surface of the powder bed (d_s), the wavelength and the time duration were fixed to 20MHz, 50 μ m, 1030nm and 500fs, respectively. To analyze the effect of the total amount of energy concerning the track length, the so called *energy per unit length* has been used (see eq. (1)) that combines the average power (P_{av}) with the scan speed.

$$Q = \frac{E_p \cdot f_{rep}}{v_{scan}} = \frac{P_{av}}{v_{scan}} \quad (1)$$

Another important quantity in ultra-short laser pulse processing is the energy density or *fluence* that is described in Eq. (2). It is used, inter alia, to determine the damage threshold of any materials that is described.

$$F = \frac{8 \cdot E_p}{\pi \cdot d_s^2} \quad (2)$$

3. Results and Discussion

Since the use of ultra-short laser pulses for SLM applications is barely investigated, yet, we present here a systematic parameter analysis.

3.1. Preliminary Investigations

In our work, ultra-short laser pulses employed as the heating source, ablation should be avoided. The single pulse ablation threshold of aluminum and silicon at 1030nm is approximately 0.12J/cm² in the sub-picosecond regime [16, 17]. The use of lower laser wavelengths would result in a linear absorption of the laser radiation by the silicon particles that strongly decreases the threshold for ablation [17]. This would lead to a higher loss of silicon and an undesirable change in the material composition at higher pulse energies

close to this threshold. Additionally, multi-pulse irradiation depending on the repetition rate leads to a reduction in the ablation threshold as well [18]. In order to analyze a possible limitation by ablation, we studied the effect of various pulse energies concerning different spot diameters on the surface of the AlSi40 powder.

We deposited a single layer with a thickness of 30 μ m on the aluminum building platform and fully scanned squares with an edge length of 2mm and a hatch distance of 1/3 of the spot diameter to ensure a suitable track overlap. At fluences higher than 0.13 J/cm² the powder was blasted away from the powder bed. This blasting threshold also slightly decreases by using higher repetition rates. Below this limit the powder was sintered and molten. The strong removal of the loose powder grains can be explained by the generation and accumulation of shockwaves combined with vaporized material that exert a very high pressure.

On the basis of this study the spot diameter was fixed to 50 μ m to use the full range of average power of the laser system up to 30W and assure a small heat affected zone to create thin structures.

3.2. Parameter Study and Microstructural Analysis

In the following experiments, the melting and sintering characteristics were analyzed whereas the repetition rate was fixed to 20MHz to ensure a proper heat accumulation of the powder particles.

At first single tracks were scanned applying an average power of 3 - 30W and energies per unit length of 50 - 1000J/m. All the tracks were separated with a minimum distance of 1mm to avoid influence from the

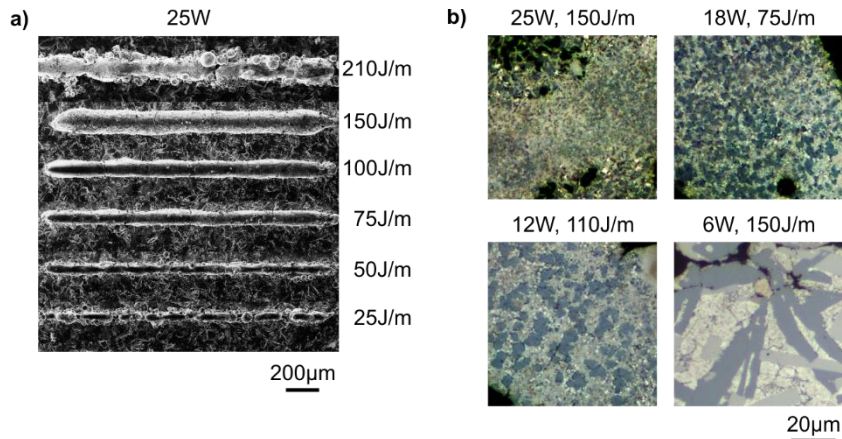


Fig. 2. (a) SEM images of molten tracks with different energies per unit length at a fixed average power of 25W and a repetition rate of 20MHz; (b) Structural analysis for different parameter settings. The dark areas represent primary silicon particles and the bright area is the surrounding α -Al and eutectic AlSi.

surrounding molten tracks and to melt the powder on pristine areas. In Fig. 2 (a) a representative selection of molten tracks at a constant average power of 25W that correspond to a pulse energy of 1.25 μ J and declining energy per unit length (increasing scan speed) is shown.

We can address various melting morphologies that give important information about the operating regime for an optimal and tailored processing. At low scanning velocities <120 mm/s ($Q > 210$ J/m) the amount of transferred heat is too high resulting in melt warps that even protrude over the powder bed. The heat flow leads to an extensive heat affected zone that is several times larger than the irradiated spot size. Track widths are in the range of 150-250 μ m with a solid, very rough top and attached partially sintered

particles. For scanning velocities larger than 800mm/s ($Q < 30\text{J/m}$) irregular structures with interruptions and droplets are formed. When additionally the average power is decreased under 6W the powder shows only surficial sintering effects (liquid phase sintering) without extensive melt formation. In an intermediate regime of about 12 - 25W and 40 - 170J/m quite uniform structures with a comparable low roughness could be melted. In this operating regime we make use of the beneficial thermal flow caused by the controlled heat accumulation of consecutive pulses.

Subsequently we studied the achievable feature sizes of additive manufactured samples in the above mentioned optimized parameter regime. We constructed single rings with a diameter of 1.5mm and built up 50 layers with a thickness of 30 μm each. The resulting thin walled hollow cylinders have an inherent high stability concerning strains along the axis. Each parameter set was complemented with a repetitive number of scans. The most homogeneous and stable formation of the walls with low porosity needed a repetitive scan of three times. After finishing and cleaning the samples in an ultrasonic bath the top of all cylinders was polished to determine the mean thickness. All the samples that couldn't stand this treatment and broke apart were not considered for further analysis. The wall thickness increases nearly linear with Q in the range of 40-150J/m and slightly increases with higher average powers. The minimal achievable, stable and reproducible feature size observed was 54 μm at 12W and 40J/m. In contrast to that the maximal thickness for this investigated regime is only 95 μm at 25W and 160J/m.

Moreover the characteristic of the phase distribution of Al and Si depending on the utilized parameters are quite important for an understanding of the mechanical properties before we can fabricate large samples for mechanical and thermal tests. Hence, the fabricated cylinders were embedded upright in epoxy and polished on the top. In Fig. 2 (b) the light microscopic images are illustrating that the primary silicon particle size (dark areas) is decreasing with increasing average power and energy per unit length. In addition, a more uniform and fine distribution of these particles surrounded by α -Al and eutectic AlSi (bright area) is observed for average powers above 15W.

3.3. Fabrication of Light-weight Samples

Based on these findings the first three-dimensional light-weight structures were realized using 25W and 125J/m ($v = 200\text{mm/s}$). Fig. 3 (a) shows a hollow hemisphere with internal supporting walls with thicknesses of 100 μm . The diameter is 8mm and it consists of 120 layers with 30 μm thickness, each. The starting angle at the bottom is 35° and it could be build up without any external supporting structures. The SEM picture on the right side clearly shows the good connection between the crossing points of the tracks. The vertical overlap of the molten layers is optimized resulting in a low porosity with only a few imperfections.

This is also confirmed by a hexagonal wall arrangement with interconnecting supporting walls (see Fig. 3 (b)). The thickness was tuned from the inside out by adding successive contour-based hatch lines with a distance of 30 μm . So we could achieve wall thicknesses from 80 to 500 μm with a slight ripple structure along

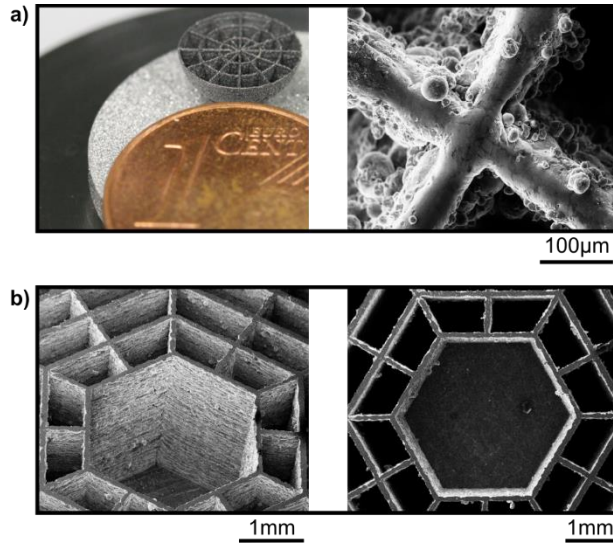


Fig. 3. (a) Hollow thin-walled hemisphere with internal support structure; (b) Hexagonal wall arrangement with radially increasing thicknesses up to 500μm and a height of 5mm.

the scanned path which can be seen by the side view of the wall. The aspect ratio achieved is 1:60 and the quality of the sub-100μm sized features is promising for future investigations.

4. Summary and Outlook

The results of these investigations clearly demonstrate the potential of using ultra-short laser pulses for additive manufacturing of material compositions like hypereutectic alloys for the fabrication of light weight structures.

A controlled heat accumulation enables a highly uniform re-solidification of the molten AlSi40 powder that is necessary for a reproducible and stable additive manufacturing. The minimal feature sizes that could be realized are close to 50μm which is the lowest value ever reported for this material composition. The microstructure formed in these thin walled samples can be controlled by tuning the average power and scan velocity to obtain fine and homogeneously distributed Si particles. Moreover first three-dimensional light-weight elements could be fabricated with aspect ratios of more than 1:60 and not supported overhangs at angles the building plate of lower than 45°.

In future work we will concentrate on the temporal and spatial shaping of the laser pulses. Defined pulse trains, so-called bursts, can be used to improve the heat transfer and to reduce thermally induced stress to avoid cracks and warps and circumvent several tedious post-processing steps. The combination of a cw laser or long pulses that heat up the material close to melting point and a subsequent activation of the phase transition with ultra-short pulses could also improve processing conditions.

Acknowledgements

We acknowledge support by the Deutsche Institut für Luft und Raumfahrttechnik (DLR) and the German Federal Ministry for Economic Affairs and Energy (BMWi) within the project ultraLEICHT (grant number 50EE1408) and the German Federal Ministry of Education and Research (BMBF) within the project AM-OPTIS (02P15B203).

References

- [1] Olakanmi, E.O., Cochrane, R.F., Dalgarno, K.W., A review on selective laser sintering/melting (SLS/SLM) of aluminum alloy powders: Processing, microstructure, and properties, *Progress in Material Science* 74, pp. 401-477 (2015).
- [2] Buchbinder, D., Schleifenbaum, H., Heidrich, S., Meiners, W., Bültmann, J., High Power Selective Laser Melting (HP SLM) of Aluminum Parts, *LIM 2011, Physics Procedia* 12, pp. 271–278 (2011).
- [3] Gebhardt, A., Kinast, J., Rohloff, R.-R., Seifert, W., Beier, M., Scheiding, S., Peschel, T., Athermal metal optics made of nickel plated AlSi40, *ICSO 2014, International Conference on Space Optics* (2014).
- [4] Zhang, L., Eskin, D.G., Miroux, A., Katgerman, L., Formation of microstructure in Al-Si Alloys under Ultrasonic Melt Treatment, in *Light Metals 2012* edited by C.E. Suarez, pp. 999-1004 (2012).
- [5] Zhao, L.Z., Zhao, M.J., Song, L.J., Mazumder, J., Ultra-fine Al-Si hypereutectic alloy fabricated by direct metal deposition, *Materials and Design* 56, pp. 542–548 (2014).
- [6] Grigoriev, S.N., Tarasova, T.V., Gvozdeva, G.O., Nowotny, S., Structure Formation of Hypereutectic Al-Si-Alloys produced by Laser Surface Treatment, *Journal of Mechanical Engineering* 60, pp. 389-394 (2014).
- [7] Grigoriev, S.N., Tarasova, T.V., Gvozdeva, G.O., Nowotny, S., Solidification behaviour during laser microcladding of Al-Si alloys, *Surface & Coatings Technology* 268, pp. 303-309 (2015).
- [8] Chichkov, B. N., Momma, C., Nolte, S., von Alvensleben, F., Tünnermann, A., Femtosecond, picosecond and nanosecond laser ablation of solids. *Appl. Phys. A* 63, 109–115 (1996).
- [9] Momma, C., Nolte, S., Chichkov, B. N., Alvensleben, F. v., Tünnermann, A., Precise laser ablation with ultrashort pulses, *Appl. Surf. Science* 109–110, pp. 15–19 (1997).
- [10] Richter, S., Döring, S., Tünnermann, A., Nolte, S., Bonding of glass with femtosecond laser pulses at high repetition rates, *Appl. Phys. A*, Vol. 103(2), pp. 257–261 (2011).
- [11] Eaton, S.M., Zhang, H., Herman, P.R., Yoshino, F., Shah, L., Bovatsek, J., Arai, A.Y., Heat accumulation effects in femtosecond laser-written waveguides with variable repetition rate, *Optics Express*, Vol. 13(12), pp. 4708-4716 (2005).
- [12] Ebert, R., Ullmann, F., Hildebrandt, D., Schille, J., Hartwig, L., Kloetzer, S., Streek, A., Exner, H., Laser Processing of Tungsten Powder with Femtosecond Laser Radiation, *JLMN-Journal of Laser Micro/Nanoengineering* Vol. 7, No. 1 (2012).
- [13] Ebert, R., Ullmann, F., Schille, J., Loeschner, U., Exner, H., Investigation of cw and ultrashort pulse laser irradiation of powder surfaces – a comparative study, *Proc. of SPIE* Vol. 8607, 86070X (2013).
- [14] Nie, B., Huang, H., Bai, S., Liu, J., Femtosecond laser melting and resolidifying of high-temperature powder materials, *Appl. Phys. A*, Vol. 118(1), pp. 37-41 (2015).
- [15] Nie, B., Yang, L., Huang, H., Bai, S., Wan, P., Liu, J., Femtosecond laser additive manufacturing of iron and tungsten parts, *Appl. Phys. A*, Vol. 119(3), pp. 1075-1080 (2015).
- [16] Gallais, L., Douti, D.-B., Commandré, M., Bataviciute, G., Pupka, E., Sciuka, M., Smalakys, L., Sirutkaitis, V., Melninkaitis, A., Wavelength dependence of femtosecond laser-induced damage threshold of optical materials, *Journal of Appl. Phys.* 177, 223103 (2015).
- [17] Harzica, R. Le, Breitling, D., Weikert, M., Sommer, S., Föhl, C., Valette, S., Donnet, C., Audouard, E., Dausinger, F., Pulse width and energy influence on laser micromachining of metals in a range of 100 fs to 5 ps, *Appl. Surf. Science* 249(1-4), pp. 322–331 (2005).
- [18] Di Niso F., Gaudio, C., Sibillano, T., Mezzapesa, F.P., Ancona, A., Lugarà, P.M., Influence of the repetition rate and pulse duration on the incubation effect in multiple-shots ultrafast laser ablation of steel, *Lasers in Manufacturing Conference 2013, Physics Procedia* 41, pp. 698-707 (2013).